The Peptide Bond Quenches Indole Fluorescence

Yu Chen, Bo Liu, Hong-Tao Yu, and Mary D. Barkley*

Contribution from the Department of Chemistry, Louisiana State University, Baton Rouge, Louisiana 70803-1804

Received April 22, 1996[⊗]

Abstract: The effect of the peptide bond on protein fluorescence is an important unresolved question in tryptophan photophysics. Definitive evidence for the peptide group as a weak quencher of indole fluorescence was obtained from solute quenching studies with a series of model compounds. Two amides are required for detectable quenching of 3-methylindole fluorescence and the quenching rate depends on the distance between amides. The bimolecular rate constants k_q of malonamide, *N*-acetylasparagine, *N*-acetylglycinamide, and *N*-acetylglutamine are 33×10^7, 8.8×10^7, 6.6×10^7, and 2.2×10^7 M^{-1} s^{-1}, respectively. Transient absorption and temperature dependence of the fluorescence lifetime measured in the absence and presence of quencher gave strong circumstantial evidence for electron transfer as the quenching mechanism. Triplet yields were measured for five indole derivatives using transient absorption. Intersystem crossing rates were calculated from triplet yield and fluorescence lifetime data. The intersystem crossing rate k_{isc} varies from 2.1×10^7 s^{-1} for 3-methylindole to 7.6×10^7 s^{-1} for indole. The peptide group does not change the value of k_{isc} of 3-methylindole. The sum of the radiative and intersystem crossing rates is equal to the temperature-independent portion of the fluorescence decay rate for 3-methylindole, indole, *N*-acetyltryptophanamide, and *N*-methylindole, confirming that intersystem crossing in indoles is independent of temperature in aqueous solution. The temperature dependence of the fluorescence lifetime of 3-methylindole was determined in the presence of *N*-acetylglycinamide, ethyl acetate, and $GdCl_3$. Two separate Arrhenius terms were resolved for water quenching and solute quenching. The activation energies for solute quenching by *N*-acetylglycinamide, ethyl acetate, and $GdCl_3$ are 2.5 ± 0.3, 0.0, and 6.0 ± 0.5 kcal/mol, respectively. For intramolecular quenching by the peptide bonds in *N*-acetyltryptophanamide, the activation energy is 3.2 ± 0.3 kcal/mol. The strategy of using the temperature dependence of the fluorescence lifetime to calculate the rates of individual nonradiative processes is discussed.

Tryptophan has been studied for more than three decades, not only because of its importance as an intrinsic fluorescent probe in proteins, but also because of its fascinating photophysical and photochemical properties. Interpretation of the complicated fluorescence decays in proteins requires thorough understanding of the multiple excited-state decay routes. Possible nonradiative processes include photoionization,[1,2] intersystem crossing,[3−5] exciplex formation,[6,7] solvent quenching,[8,9] excited-state proton transfer,[10−14] excited-state electron transfer,[15,16] as well as internal conversion. Usually two or more processes contribute to the nonradiative rate of the indole chromophore and each process may depend differently on environment. Thus, it is essential to devise ways to measure each process separately.

Photoionization[1] and intersystem crossing[4] have been observed in flash photolysis experiments. Photoionization occurs from a prefluorescent state, and therefore affects the fluorescence quantum yield but not the lifetime. The concept of exciplex was introduced by Lumry and co-workers with indole as the first example.[6] Exciplex formation may be the mechanism underlying solvent quenching and electron transfer. Solvent quenching and excited-state proton transfer depend on solvent isotope and temperature. Water quenching occurs in all indoles with a large activation energy around 11−13 kcal/mol.[9] Intramolecular excited-state proton transfer from the amino group of tryptophan to the C-4 position on the indole ring was demonstrated by Saito et al.[12] using H−D exchange experiments. Intermolecular excited-state proton transfer also happens at aromatic carbons when the indole chromophore comes in contact with strong proton donors.[14,17] Excited-state electron transfer has been inferred from the correlation between bimolecular quenching rate and reduction potential of solute quenchers.[18]

Several fundamental questions remain about tryptophan fluorescence that are especially pertinent to proteins. (1) Does

[⊗] Abstract published in *Advance ACS Abstracts,* September 15, 1996.

(1) Amouyal, E.; Bernas, A.; Grand, D.; Mialocq, J.-C. *Faraday. Discuss. Chem. Soc.* **1982**, *74*, 147−159.
(2) Mialocq, J. C.; Amouyal, E.; Bernas, A.; Grand, D. *J. Phys. Chem.* **1982**, *86*, 3173−3177.
(3) Santus, R.; Grossweiner, L. I. *Photochem. Photobiol.* **1972**, *15*, 101−105.
(4) Bent, D. V.; Hayon, E. *J. Am. Chem. Soc.* **1975**, *97*, 2612−2619.
(5) Grossweiner, L. I.; Brendzel, A. M.; Blum, A. *Chem. Phys.* **1981**, *57*, 147−155.
(6) Walker, M. S.; Bednar, T. W.; Lumry, R. *J. Chem. Phys.* **1966**, *45*, 3455−3456.
(7) Lasser, N.; Feitelson, J.; Lumry, R. *Isr. J. Chem.* **1977**, *16*, 330−334.
(8) Lee, J.; Robinson, G. W. *J. Chem. Phys.* **1984**, *81*, 1203−1208.
(9) McMahon, L. P.; Colucci, W. J.; McLaughlin, M. L.; Barkley, M. D. *J. Am. Chem. Soc.* **1992**, *114*, 8442−8448.
(10) Stryer, L. *J. Am. Chem. Soc.* **1966**, *88*, 5708−5712.
(11) Robbins, R. F.; Fleming, G. R.; Beddard, G. S.; Robinson, G. W.; Thistlewaite, P. J.; Woolfe, G. J. *J. Am. Chem. Soc.* **1980**, *102*, 6271−6279.
(12) Saito, I.; Sugiyama, H.; Yamamoto, A.; Muramatsu, S.; Matsuura, T. *J. Am. Chem. Soc.* **1984**, *106*, 4286−4287.
(13) Shizuka, H.; Serizawa, M.; Shimo, T.; Saito, I.; Matsuura, T. *J. Am. Chem. Soc.* **1988**, *110*, 1930−1934.
(14) Yu, H.-T.; Colucci, W. J.; McLaughlin, M. L.; Barkley, M. D. *J. Am. Chem. Soc.* **1992**, *114*, 8449−8454.
(15) Werner, T. C.; Forster, L. S. *Photochem. Photobiol.* **1978**, *29*, 905−914.
(16) Petrich, F. W.; Chang, M. C.; McDonald, D. B.; Fleming, G. R. *J. Am. Chem. Soc.* **1983**, *105*, 3824−3832.
(17) Chen, Y.; Liu, B.; Barkley, M. D. *J. Am. Chem. Soc.* **1995**, *117*, 5608−5609.
(18) Steiner, R. F.; Kirby, E. P. *J. Phys. Chem.* **1969**, *73*, 4130−4135.

S0002-7863(96)01307-8 CCC: $12.00

the peptide bond quench indole fluorescence? Ricci and Nesta[19] reported that acetamide has no detectable quenching effect, whereas Froehlich and Nelson[20] showed that an electron-withdrawing substituent such as chlorine makes the quenching efficient. However, the electron-withdrawing group may also introduce another decay pathway. In most experiments with small peptides,[15,21] other quenching groups such as ammonium were present, complicating the interpretation. (2) Does electron transfer occur from the excited indole ring to an electrophilic acceptor? Electron transfer has been proposed as a major nonradiative pathway of tryptophan[16] and the main quenching event in proteins. But the evidence is indirect and the distance and temperature dependence are unknown. (3) Are there other temperature-dependent nonradiative channels in indole derivatives besides solvent quenching and proton transfer? A second weak temperature-dependent process has been invoked to account for the lower apparent activation energy in *N*-acetyltryptophanamide (NATA) and *N*-acetyltryptophan ethyl ester compared to indole or 3-methylindole. (4) Is intersystem crossing sensitive to environment?

The present paper addresses these questions using a simple model system comprised of 3-methylindole and various solute quenchers. Stern−Volmer quenching experiments with a series of model compounds containing one or two primary or secondary amides show that the peptide bond quenches indole fluorescence. We investigate the mechanism of this quenching process and devise ways of separating it from other nonradiative processes. Triplet yields are measured by transient absorption experiments in the absence and presence of quenchers and intersystem crossing rates are calculated. The temperature dependence of the quenching process is also determined. The contribution of this process to the overall fluorescence decay rate is estimated from the Arrhenius parameters. Finally, we discuss the application of these results to proteins.

Experimental Section

Chemicals. 3-Methylindole (3-MeIn), *N*-methylindole, and NATA were bought from Aldrich and used without further purification. Indole and tryptophan from Sigma were recrystallized four times from 70% ethanol. *N*-Acetylglycinamide (NAGA) from Aldrich and *N*-acetyl-*N*-methylglycinamide (*N*-Me-NAGA) and *N*-acetylprolinamide from Sigma were recrystallized from 2:3 v/v methanol−hexanes. Other chemicals (highest grade) from Sigma or Aldrich were used as received.

Steady-state and time-resolved fluorescence measurements have been described elsewhere.[9] All fluorescence measurements were made with excitation wavelength of 288 nm on solutions of absorbance <0.1. Fluorescence quantum yields Φ_F were measured relative to tryptophan using a value of 0.14 in water at 25 °C. Stern−Volmer quenching constants were determined from relative quantum yields. The time-correlated single photon counting instrument was equipped with a thermoelectrically cooled Hamamatsu R2809U microchannel plate photomultiplier and had an instrumental response of 100 ps fwhm. Fluorescence lifetimes τ were measured at 370 or 390 nm emission wavelength (8-nm bandpass). Decay data were acquired contemporaneously from a fluorescent sample and a solution of coffee creamer in water for the instrumental response. Decay curves were stored in 1024 channels of 6−81 ps/channel. The decay data were deconvolved over channels 1−1024 in the Beechem global program.[22] The quality of the fit was judged by reduced χ_r^2, weighted residuals, and autocorrelation function of the weighted residuals. The radiative rate k_r was derived from $k_r = \Phi_F/\tau$. Lifetime data acquired as a function of temperature were also deconvolved directly in a global analysis assuming one or two temperature-dependent terms. χ_r^2 values were in the range of 1.1−1.5 for single curve analyses, somewhat higher for global analyses.

Laser flash photolysis experiments were carried out at the Louisiana State University Center for Advanced Microstructures and Devices. A Spectra-Physics GCR-5 Q-switched Nd:YAG laser was frequency doubled using a temperature-controlled KDP crystal. The output beam pumped a Spectra-Physics PDL-3 dye laser with rhodamine 6G. The dye laser output was passed through a Spectra-Physics wavelength extension system containing a KDP crystal to frequency double into the UV. An excitation wavelength of 280 nm was selected. The laser has a 10 Hz repetition rate with pulse duration of about 6 ns and power up to 30 mJ/pulse. The excitation light was <0.8 mJ/pulse to prevent multiphotonic processes. The beam was 8-mm square and nonuniform. A cylindrical lens was used to compress the vertical dimension to match the probe beam. The stability of the 280-nm output usually varied about 7% over a day monitored either by an Astral-AD30 power meter or a photodiode. The monitor light source was a 75-W xenon lamp with a Photon Technology Inc. LPS-220 power supply. White light was passed through the sample and a SPEX M220 monochromator and was detected with an Action Research Corp. PD-439 photomultiplier. The signal was displayed on a Tektronix TDS 520 digital oscilloscope and transferred to an IBM 386 PC for analysis. The time response of the detection system is about 30−50 ns.

Transient absorption measurements were made on $1-2 \times 10^{-4}$ M ($A_{280} = 0.6-0.8$) solutions in 1-cm cells at ∼25 °C. Solutions were deoxygenated by bubbling oxygen-free N_2 gas through the cell. Initial absorbance is determined by extrapolation of the transient absorbance $OD(t) = \log[I_o/I(t)]$ to $t = 0$. The short laser pulse permits accurate measurements of initial absorbance, avoiding corrections for triplet decay kinetics. The absorbance of the triplet at 460 nm also contains contributions from solvated electron and neutral radical. The absorbance of solvated electron at 680 nm is measured and used to calculate the contribution at 460 nm based on the published absorption spectrum.[23] A contribution of 0.20 OD_{680nm} from solvated electron is subtracted from the total absorbance at 460 nm. This procedure gave about the same absorbance at 460 nm for 3-methylindole as the usual method of adding butanol plus 1 atm of N_2O to scavenge solvated electrons. Two methods are used to estimate the absorbance of the neutral radical at 460 nm: (1) fitting the transient absorbance to double or triple exponential functions and (2) extrapolating a log plot of the transient absorbance at long times to $t = 0$. The neutral radical has been proposed to be the long-lifetime component.[4] The initial absorbance of the neutral radical is calculated from the amplitude of the long-lifetime component and subtracted from the total absorbance. The transient absorbance of the cation radical is monitored at 580 nm in the presence of l atm of N_2O and 0.2 M 2-propanol to scavenge solvated electrons.[3,4]

Triplet quantum yields were determined using a fluorescence quencher, iodide, that increases the intersystem crossing rate.[24,25] The triplet absorbance as a function of KI concentration is

$$OD_T/OD^\circ_T = (1 + k_q[KI]/k_{isc})/(1 + k_q\tau_{o,deox}[KI]) \qquad (1)$$

where OD_T and OD°_T are the triplet absorbance in the presence and absence of iodide, k_q is the fluorescence quenching rate constant assuming that the only quenching process is intersystem crossing, k_{isc} is the intersystem crossing rate in the absence of iodide, and $\tau_{o,deox}$ is the fluorescence lifetime in the absence of iodide measured in deoxygenated solution. Rearranging eq 1 gives

$$[KI]/(OD_T/OD^\circ_T - 1) = \Phi_T\,[(OD_T/OD^\circ_T)/(OD_T/OD^\circ_T - 1)][KI] + k_{isc}/k_q \qquad (2)$$

The triplet yield Φ_T is obtained from the slope of a plot of $[KI]/(OD_T/OD^\circ_T - 1)$ *vs* $[(OD_T/OD^\circ_T)/(OD_T/OD^\circ_T - 1)][KI]$. It can also be shown from eq 1 that as $[KI] \rightarrow \infty$

(19) Ricci, R. W.; Nesta, J. M. *J. Phys. Chem.* **1976**, *80*, 974−980.
(20) Froehlich, P. M.; Nelson, K. *J. Phys. Chem.* **1978**, *82*, 2401−2403.
(21) Cowgill, R. W. *Biochim. Biophys. Acta* **1970**, *200*, 18−25.
(22) Beechem, J. M. *Chem. Phys. Lipids* **1989**, *50*, 237−251.
(23) Keene, J. P. *Radia. Res.* **1964**, *22*, 1−13.
(24) Medinger, T.; Wilkinson, F. *Trans. Faraday Soc.* **1965**, *61*, 620−630.
(25) Vander Donckt, E.; Lietaer, D. *Trans. Faraday Soc.* **1971**, 112−120.

$$(OD_T/OD°_T) = 1/(k_{isc}\tau_{o,deox}) = 1/\Phi_T \quad (3)$$

Fluorescence lifetime measurements on deoxygenated samples were made immediately after bubbling oxygen-free N_2 gas through the cell for 10 min and sealing the cell with a Teflon stopper. The intersystem crossing rate is derived from

$$k_{isc} = \Phi_T/\tau_{o,deox} \quad (4)$$

Results and Discussion

Fluorescence Quenching. Three classes of compounds were examined to clarify the quenching ability of amide, carboxylate, and peptide groups. The first class containing one amide includes acetamide, *N*-methylacetamide, *N*,*N*-dimethylacetamide (DMA), and *N*-methylpropionamide. The second class containing one peptide and one carboxylate or containing two carboxylates includes *N*-acetylglycine, *N*-acetylalanine, *N*-acetylleucine, *N*-acetylvaline, *N*-acetylproline, *N*-acetylserine, *N*-acetylmethionine, malonate, and succinate. The third class containing two amides or containing one amide and one peptide includes malonamide, *N*-acetylglycinamide, *N*-Me-NAGA, *N*-acetylprolinamide, *N*-acetylglutamine, and *N*-acetylasparagine. Quenching of 3-methylindole fluorescence was measured at 25 °C in aqueous solutions at pH 7−8. Bimolecular quenching rate constants k_q were derived from the slope of a Stern−Volmer plot, $\Phi_o/\Phi = 1 + k_q\tau_o[Q]$. Φ_o and Φ are the fluorescence quantum yield in the absence and presence of quencher, and τ_o is the lifetime in the absence of quencher.

There was no detectable quenching of 3-methylindole fluorescence by the first two classes of compounds, in agreement with the previous result for acetamide.[19] Rather, addition of these compounds caused small increases of quantum yield and lifetime. This is probably due to the decreased water activity and slower water quenching rate.[8,9] On the other hand, the compounds in class three definitely quench 3-methylindole fluorescence, albeit with low quenching rate constants (Table 1). The lifetime and quantum yield drops were equal, indicating that the quenching is due to an increase in the total nonradiative rate. Clearly amide is a weak quenching group, because at least two amides are necessary for detectable quenching. The amide group is a better quencher than carboxylate, because two carboxylates or one carboxylate and one amide do not cause detectable quenching. The class three compounds have quenching rates from 2.2×10^7 M^{-1} s^{-1} for *N*-acetylglutamine to 33×10^7 M^{-1} s^{-1} for malonamide. The lower quenching rate of *N*-acetylglutamine is probably due to the greater distance between the two amide groups compared to the other compounds.

An electron transfer mechanism has been proposed to account for amide quenching, where the indole ring acts as an electron donor, the carbonyl group acts as an electron acceptor, and quenching occurs via a "charge transfer stabilized exciplex".[20] Several other quenching mechanisms are readily ruled out. The absorption and emission spectra of 3-methylindole did not change in the presence of quencher, indicating no ground-state complexation. Resonance energy transfer can be excluded because there is no overlap of the 3-methylindole emission and amide absorption spectra. Excited-state proton transfer either from amide hydrogen to the indole ring or from indole NH to amide is unlikely because the amide group is a very weak acid/base and the deuterium isotope effect on k_q is insignificant (Table 1). However, enhancement of intersystem crossing and internal conversion remain as possible quenching mechanisms. Consequently, we looked at the effect of the peptide bond on the intersystem crossing rate by measuring the triplet yield.

Table 1. Bimolecular Quenching Rate Constants for 3-Methylindole

quencher	solvent	Stern−Volmer k_q[a] (10^{-7} M^{-1} s^{-1})	temperature study k_q[b] (10^{-7} M^{-1} s^{-1})
NAGA	H_2O	6.6	4.5
NAGA	D_2O	6.5	5.5
N-Me-NAGA	H_2O	5.9	
N-acetylprolinamide	H_2O	6.2	
N-acetylasparagine	H_2O[c]	8.8	
N-acetylglutamine	H_2O[c]	2.2	
malonamide	H_2O	33	
ethyl acetate	H_2O	17	14
ethyl acetate	D_2O	20	15
$GdCl_3$	H_2O	14	16
$GdCl_3$	D_2O	6.0	6.3
KI	H_2O	130	

[a] The lifetime of 3-methylindole is 8.2 ns in H_2O and 12.0 ns in D_2O at 25 °C, oxygenated solution. [b] Calculated using eq 10 from data in Table 3. [c] pH 7 adjusted with NaOH.

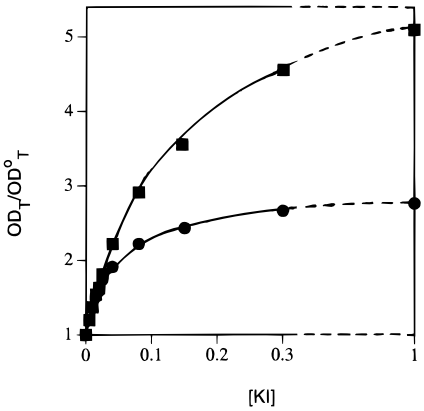

Figure 1. Relative triplet yield of (■) 3-methylindole and (●) indole as a function of [KI] at room temperature.

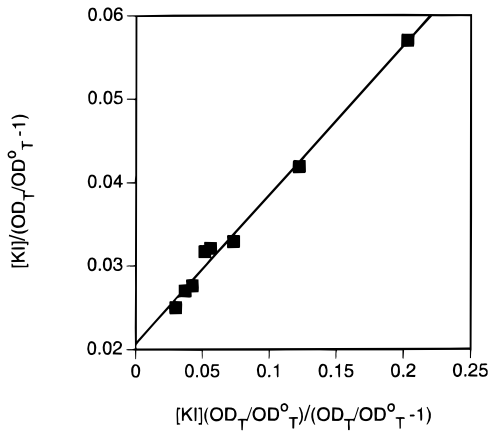

Figure 2. Data for 3-methylindole from Figure 1 plotted according to eq 2. [KI] = 0.005−0.15 M. The line is the linear regression with the slope equal to Φ_T.

Transient Absorption. To our knowledge, the triplet yield of 3-methylindole has not been measured in aqueous solution. We used the method of Medinger and Wilkinson[24] as modified by Vander Donckt and Lietaer[25] to determine the triplet yield of 3-methylindole. For comparison with literature values, we also measured the triplet yield of indole, *N*-methylindole, NATA, and tryptophan. Figure 1 plots the triplet absorbance *vs* KI concentration for 3-methylindole and indole. At high concentration of KI, the absorbance reaches a plateau (eq 3). Figure 2 shows a plot of the 3-methylindole data according to eq 2. The plot of $[Q]/(OD_T/OD°_T - 1)$ *vs* $(OD_T/OD°_T)/(OD_T/OD°_T - 1)[Q]$ is linear with slope equal to the triplet yield Φ_T.

Table 2. Triplet Quantum Yield and Intersystem Crossing Rate of Indoles in the Absence and Presence of Quenchers

compd	$\tau_{o,deox}$(ns)[a]	Φ_T[b] eq 2	Φ_T[b] eq 3	Φ_T lit.	k_{isc} (10^7 s^{-1})	k_r (10^7 s^{-1})	$k_r + k_{isc}$ (10^7 s^{-1})	k_o[c] (10^7 s^{-1})
3-methylindole	8.7	0.18	0.18	0.17[11]	2.1	4.2[14]	6.3	6.0
indole	4.4	0.35	0.32	0.23[28]	7.6	5.9	13.5	13.9[33]
N-methylindole	8.5	0.34	0.31	0.33[40]	4.0	5.7[14]	9.7	10.3[9]
NATA	3.0	0.15	0.15	0.21[26]	5.0	5.8	10.8	9.8
tryptophan	2.6(ave)	0.14	0.12	0.10[11]	5.0	5.3	10.3	
3-MeIn + 0.8 M NAGA	6.6	0.13			2.0			
3-MeIn + 0.16 M CH_3COOEt	6.9	0.14			2.0			
3-MeIn + 0.5 M $GdCl_3$	5.7	0.18			3.2			

[a] 25 °C, deoxygenated solution. [b] Estimated error ±10%. [c] k_o is temperature-independent rate in eq 6.

Analyses according to eqs 2 and 3 give the same values of Φ_T (Table 2). The triplet yields of 3-substituted indoles are 2-fold smaller than the yields for indole and *N*-methylindole. Volkert et al.[26] determined the triplet yield of NATA and tryptophan in aqueous solution by the method of Medinger and Wilkinson.[24] Their values of 0.21 and 0.18 for NATA and tryptophan, respectively, obtained using bromide as quencher are 0.06 unit higher than our values using iodide. This method for determining the triplet yield assumes that intersystem crossing is the only nonradiative process affected by the heavy-atom quencher. The triplet yield will be overestimated if other nonradiative processes are introduced or enhanced. For bromide quenching of tryptophan fluorescence, acceleration of intersystem crossing is the major, but not the only, pathway affected by bromide.[27] Robbins et al.[11] derived $\Phi_T = 0.17$ for 3-methylindole from the fluorescence quantum yield at low temperature assuming $\Phi_F + \Phi_T = 1$, which is very close to our value. Klein et al.[28] determined $\Phi_T = 0.43$ for indole in cyclohexane by the energy transfer method. Assuming that oscillator strengths are independent of solvent, they estimated $\Phi_T = 0.23$ in aqueous solution. Approximations made by Klein et al.[28] in determining the triplet extinction coefficient and initial triplet absorbance may explain the discrepancy with the value in Table 2.

Intersystem crossing rates k_{isc} were derived according to eq 4 from triplet yields and fluorescence lifetimes $\tau_{o,deox}$ measured under deoxygenated conditions. The value of $\tau_{o,deox}$ was a few percent larger compared to oxygenated solution. The intersystem crossing rates ranged from 2.1×10^7 s^{-1} for 3-methylindole to 7.6×10^7 s^{-1} for indole (Table 2). Intersystem crossing rates have been measured for 3-methylindole, indole, and *N*-methylindole in the gas phase.[29] The gas-phase value of 2.5×10^7 s^{-1} for 3-methylindole is very close to the solution value. However, intersystem crossing rates of $1.7-2.4 \times 10^7$ s^{-1} for indole and $1.8-2.3 \times 10^7$ s^{-1} for *N*-methylindole in the gas phase are slower than the rates in aqueous solution. Knowing the value of k_{isc}, we can go back and estimate the fluorescence quenching rate constant k_q for iodide by curve fitting the data in Figure 1 to eq 1 or by using eq 2 with the intercept of the plot in Figure 2. The k_q value for 3-methylindole calculated in this way is 1.1×10^9 M^{-1} s^{-1}, which is in good agreement with the value from the Stern−Volmer plot (Table 1). This suggests that intersystem crossing is the only nonradiative process affected by iodide, validating the use of this method for measuring the triplet yield.

The relative triplet yield $\Phi_{T,Q}$ of 3-methylindole in the presence 0.8 M NAGA was determined from initial triplet absorbance measurements

$$\Phi_{T,Q} = [OD^\circ_{T,Q}/OD^\circ_T]\,\Phi_T \qquad (5)$$

where $OD^\circ_{T,Q}$ and OD°_T are the initial absorbance measured in the presence and absence of NAGA. The triplet yield Φ_T of 3-methylindole dropped 30% in the presence of 0.8 M NAGA (Table 2). The intersystem crossing rate was derived from eq 4, where $\tau_{o,deox}$ was measured in the presence of 0.8 M NAGA. While NAGA decreases Φ_T, it has no effect on k_{isc} within experimental error. Thus, NAGA does not quench 3-methylindole fluorescence by increasing the intersystem crossing rate. This implies that the quenching mechanism is excited-state electron transfer or enhancement of internal conversion.

We also looked at two other types of quenchers, ester and metal ion, which have been proposed to quench indole fluorescence by electron transfer.[19,30] As in the case of NAGA, 0.16 M ethyl acetate decreases the triplet yield, but does not affect the intersystem crossing rate (Table 2). In the presence of 0.5 M $GdCl_3$, however, the triplet yield does not change and the intersystem crossing rate increases. The bimolecular rate constant for producing triplet by Gd^{3+} is $k^\circ_q = (3.2 - 2.1) \times 10^7$ $s^{-1}/[Gd^{3+}] = 2.2 \times 10^7$ M^{-1} s^{-1}, which is much lower than the fluorescence quenching constant $k_q = 14.0 \times 10^7$ M^{-1} s^{-1}. Clearly, triplet production is only a minor quenching pathway of Gd^{3+}. Two other quenching mechanisms are possible for Gd^{3+}: excited-state electron transfer and excited-state proton transfer. The p*K* of aquated Gd^{3+} is 8.2 in H_2O and 8.3 in D_2O,[31] so in principle $[Gd(H_2O)_6]^{3+}$ could donate a proton to excited indole. We should keep in mind, therefore, that some quenchers may have more than one quenching pathway.

Transient absorption spectra of the five indole derivatives were also monitored in the presence of the quenchers. The primary photoproducts of indoles are proposed to be triplet, neutral radical, cation radical, and solvated electron.[3,4] The solvated electron at 680 nm is quenched by all these compounds. The cation radical at 580 nm is also quenched. The neutral radical at 520 nm is not sensitive to the quenchers, although the cation radical is completely gone. $GdCl_3$ caused a new absorption band at around 570 nm with long decay time similar to neutral radical. A detailed study will be published elsewhere. This new species is presumed to be an exciplex.

Temperature Dependence. The temperature dependence of the fluorescence lifetime splits the nonradiative rate into temperature-independent and temperature-dependent contributions. In most aromatic chromophores, the internal conversion rate k_{ic} is independent of temperature.[32] We have already characterized the temperature dependence of water quenching

(26) Volkert, W. A.; Kuntz, R. R.; Ghiron, C. A.; Evans, R. F. *Photochem. Photobiol.* **1977**, *26*, 3−9.
(27) Evans, R. F.; Kuntz, R. R.; Volker, W. A.; Ghiron, C. A. *Photochem. Photobiol.* **1978**, *27*, 511−515.
(28) Klein, R.; Tatischeff, I.; Bazin, M.; Santus, R. *J. Phys. Chem.* **1981**, *85*, 670−677.
(29) Lipert, R. J.; Bermudez, G.; Colson, S. D. *J. Phys. Chem.* **1988**, *92*, 3801−3805.
(30) Ricci, R. W.; Kilichowski, K. B. *J. Phys. Chem.* **1974**, *76*, 1953−1956.
(31) Amaya, T.; Kakihana, H.; Maeda, M. *Bull. Chem. Soc. Jpn.* **1973**, *46*, 2889−2890.

Table 3. Arrhenius Parameters of 3-Methylindole in H_2O and D_2O in the Presence of Control Compounds and Quenchers

compd	analysis procedure	k_o, k'_o (10^7 s^{-1})	A_1 (s^{-1})	E^*_1 (kcal/mol)	k_{si} (10^7 s^{-1})	A_2 (M^{-1} s^{-1})	E^*_2 (kcal/mol)	χ_r^2
			3-Methylindole					
H_2O	I	6.0	1.2×10^{17}	12.7	5.9			1.2
H_2O, 1.7 M DMA	I	6.8	7.3×10^{15}	11.3	3.8			1.6
D_2O, 1.0 M DMA	I	6.3	2.2×10^{16}	12.4	1.8			1.5
H_2O, 0.5 M EtOH	I	6.5	2.5×10^{16}	11.8	5.4			1.5
D_2O, 0.5 M EtOD	I	5.8	3.6×10^{16}	12.6	2.1			1.8
H_2O, 2.0 M KCl	I	6.5	3.4×10^{16}	12.1	4.6			1.6
D_2O, 2.0 M KCl	I	5.8	2.7×10^{16}	12.6	1.5			1.4
H_2O, 1.7 M NAGA	I	11.9	1.6×10^{15}	10.1	6.3			2.0
D_2O, 1.0 M NAGA	I	10.0	2.8×10^{15}	11.0	2.4			2.2
H_2O, 1.7 M NAGA	I[a]	13.4	4.2×10^{15}	10.9	4.3			9.8
D_2O, 1.0 M NAGA	I[a]	11.0	1.1×10^{16}	11.9	2.1			3.9
H_2O, 1.7 M NAGA	II	7.3	7.3×10^{15}	11.3	3.8	2.8×10^9	2.5 ± 0.3	1.8
D_2O, 1.0 M NAGA	II	7.6	1.7×10^{16}	12.3	1.6	5.0×10^9	2.8 ± 0.3	2.0
H_2O, 0.5 M CH_3COOEt	I, I[a]	13.1	2.5×10^{16}	11.8	5.5			1.5
D_2O, 0.5 M CH_3COOEt	I, I[a]	13.2	3.2×10^{16}	12.5	2.1			2.0
H_2O, 1.0 M $GdCl_3$	I	12.2	7.7×10^{14}	9.1	16.2			2.1
D_2O, 1.0 M $GdCl_3$	I	8.7	1.1×10^{15}	9.9	6.0			2.0
H_2O, 1.0 M $GdCl_3$	I[a]	18.0	4.7×10^{15}	10.6	6.9			80
D_2O, 1.0 M $GdCl_3$	I[a]	12.0	7.8×10^{15}	11.6	2.4			43
H_2O, 1.0 M $GdCl_3$	II	8.8 ± 0.5	3.4×10^{16}	12.1	5.0	3.7×10^{12}	6.0 ± 0.5	1.9
D_2O, 1.0 M $GdCl_3$	II	7.7 ± 0.5	3.3×10^{16}	12.5	2.2	2.2×10^{12}	6.4 ± 0.5	2.0
			NATA					
H_2O	I	17	2.2×10^{13}	6.9	19.0			2.4
D_2O	I	15	2.3×10^{13}	5.7	15.0			2.0
H_2O	II	9.8 ± 1.0	6.0×10^{16}	12.6	3.4	4.5×10^{10} s^{-1}	3.2 ± 0.3	1.9
D_2O	II	7.9 ± 0.7	2.1×10^{16}	12.6	1.2	4.8×10^{10} s^{-1}	3.2 ± 0.3	1.5

[a] Data sets for quencher and control compound were linked.

and excited-state proton transfer in indoles. Here we determine the temperature dependence of quenching by the peptide bond and other putative electron acceptors. Fluorescence lifetimes were measured in H_2O and D_2O as a function of temperature from 5 to 60 °C in the presence of the three types of quenchers; 1.7 M NAGA, 0.5 M ethyl acetate, and 1.0 M $GdCl_3$ were added to quench 3-methylindole fluorescence by 50% at 25 °C. At these concentrations, added solutes will affect the water quenching rate.[8] For example, the quantum yield and lifetime of 3-methylindole in H_2O increased almost 10% in the presence of 1.7 M DMA at 25 °C. In order to correct for decreases in water quenching, parallel experiments were performed using 1.7 M DMA, 0.5 M ethanol, and 2.0 M KCl as control compounds for 1.7 M NAGA, 0.5 M ethyl acetate, and 1.0 M $GdCl_3$. The fluorescence decay of 3-methylindole is monoexponential in the presence of the control compounds and quenchers.

The temperature dependence of the fluorescence lifetime of 3-methylindole in the presence of control compounds and quenchers can be expressed by Arrhenius factors.

$$1/\tau_c = k_o + A_1 \exp(-E^*_1/RT) \quad (6)$$

$$1/\tau_q = k_o' + A_1 \exp(-E^*_1/RT) + A_2[Q] \exp(-E^*_2/RT) \quad (7)$$

Here τ_c is the lifetime of 3-methylindole with control compound and τ_q is the lifetime with quencher. k_o is the total temperature-independent rate without quencher. Presumably $k_o = k_r + k_{ic} + k_{isc}$, where k_{ic} is the internal conversion rate. $k_o' = k_o + k^\circ_q[Q]$, where k°_q is the temperature-independent rate caused by the quencher. The first Arrhenius term $A_1 \exp(-E^*_1/RT)$ represents water quenching. The second Arrhenius term $A_2[Q] \exp(-E^*_2/RT)$ gives the temperature dependence of the quenching process. The temperature dependence of the fluorescence decay data was analyzed by three procedures.

(32) Birks, J. B. *Photophysics of Aromatic Molecules*; Wiley: New York, 1970; p 146.

Procedure I fits the fluorescence decay curves in a global analysis assuming one temperature-dependent term as in eq 6.

$$I(t) = \alpha \exp[-t\{k_o + A_1 \exp(-E^*_1/RT)\}] \quad (8)$$

The temperature data sets with control compounds always gave acceptable fits to eq 8 with $\chi_r^2 = 1.2-1.6$. The temperature-independent rate k_o and activation energy E^*_1 are slightly different in H_2O and D_2O (Table 3). Simultaneous analysis of the H_2O and D_2O data sets with E^*_1 linked gives $\chi_r^2 = 1.8-2.1$. If both k_o and E^*_1 are linked in the global analysis, the fits are much worse with $\chi_r^2 = 4.1-5.7$. Apparently, the k_o values differ by $(0.5-0.7) \times 10^7$ s^{-1} in H_2O and D_2O in the presence of the control compounds. This is not due to a solvent isotope effect on the radiative rate: $k_r = 4.4 \times 10^7$ s^{-1} in H_2O and 4.3×10^7 s^{-1} in D_2O in the presence of 2 M KCl. The deuterium isotope effect on k_o may be due to a decrease in k_{isc} or k_{ic} in D_2O relative to H_2O. The water quenching rates were calculated from $k_{si} = A_1 \exp(-E^*_1/RT)$ at 25 °C. The added solute depresses water quenching somewhat (Table 3). Analysis of the data sets for NAGA and $GdCl_3$ gave $\chi_r^2 = 2.0-2.1$ with higher values for k_{si} than the control compounds. The data set for ethyl acetate gave the same χ_r^2 and k_{si} values as the ethanol control. Quenchers and control compounds should cause similar changes in the water quenching rate. This assumption was tested by simultaneous analysis of the data sets for quencher and control compound with the activation energy E^*_1 and frequency factor A_1 linked in the global analysis (analysis procedure I[a] in Table 3). The fits are very poor for NAGA and Gd^{3+}, but acceptable for ethyl acetate. This implies that the quenching of 3-methylindole fluorescence by NAGA and Gd^{3+} is temperature dependent. The Arrhenius parameters obtained when the NAGA and Gd^{3+} data sets are analyzed separately from the control would be distorted by a second temperature-dependent process. In the case of ethyl acetate, however, the values of χ_r^2, A_1, and E^*_1 are the same for global analyses with and without the ethanol control, indicating that

ethyl acetate quenches by a temperature-independent process resulting in an increase in k_o.

Procedure II fits the fluorescence decay curves in the presence of quenchers assuming two temperature-dependent terms as in eq 7.

$$I(t) = \alpha \exp[-t\{k'_o + A_1 \exp(-E^*_1/RT) + A_2[Q] \exp(-E^*_2/RT)\}] \quad (9)$$

The first temperature-dependent term corresponds to water quenching. The A_1 and E^*_1 parameters were linked in global analyses of the temperature data sets for quencher and control compound. The results are given in Table 3. Only one temperature-dependent term could be resolved for ethyl acetate. For NAGA and Gd^{3+}, the k'_o, A_2, and E^*_2 values obtained were sensitive to initial guess. The transient absorption studies showed that NAGA does not affect the intersystem crossing rate. Therefore, the NAGA and DMA data sets were also analyzed together linking k_o, A_1, and E^*_1. The Arrhenius parameters for the second temperature-dependent process, $A_2 = 2.8 \times 10^9$ M^{-1} s^{-1} and $E^*_2 = 2.2$ kcal/mol in H_2O, were within experimental error of the values obtained from the analysis without linking k_o (Table 3). Thus, quenching of 3-methylindole fluorescence by NAGA is weakly temperature dependent. The temperature dependence of Gd^{3+} quenching is considerably stronger with $A_2 = 3.7 \times 10^{12}$ M^{-1} s^{-1} and $E^*_2 = 6.0 \pm 0.5$ kcal/mol in H_2O. The recovered k'_o value of $8.8 \pm 0.5 \times 10^7$ s^{-1} is higher than the KCl control. The increase in the temperature-independent rate $k^\circ_q = (8.8-6.5) \times 10^7$ s^{-1}/$[Gd^{3+}] = 2.3 \times 10^7$ M^{-1} s^{-1} due to Gd^{3+} is close to the value of 2.2×10^7 M^{-1} s^{-1} derived from transient absorption experiments. These results confirm that Gd^{3+} quenches by more than one mechanism, one of which is enhancement of the temperature-independent intersystem crossing rate. The overall bimolecular quenching rate constant can be calculated from the Arrhenius parameters.

$$k_q = k^\circ_q + A_2 \exp(-E^*_2/RT) \quad (10)$$

The k_q values from temperature studies are in good agreement with the values from Stern−Volmer plots (Table 1). Therefore, procedure II provides a way to measure the rates of two processes with distinct activation energies from fluorescence lifetime data.

Procedure III is a two-step method for analyzing the temperature dependence of the fluorescence lifetime. Subtracting eq 6 from eq 7 gives

$$1/\tau_q - 1/\tau_c = k^\circ_q [Q] + A_2[Q] \exp(-E^*_2/RT) \quad (11)$$

Figure 3a is the plot of $1/\tau_q - 1/\tau_c$ *vs* $1/T$ for NAGA, ethyl acetate, and Gd^{3+} in H_2O. For ethyl acetate, the plot is almost a horizontal line, indicating that the quenching is temperature independent or very slightly temperature dependent. k°_q can be estimated from the average value of $1/\tau_q - 1/\tau_c$ or from the intercept of the plot. The value of $(1.5-1.6) \times 10^8$ M^{-1} s^{-1} is similar to the Stern−Volmer quenching constant $k_q = 1.7 \times 10^8$ M^{-1} s^{-1}. The plots of $1/\tau_q - 1/\tau_c$ *vs* $1/T$ for NAGA and Gd^{3+} are curved, suggesting that the second temperature-dependent term $A_2[Q] \exp(-E^*_2/RT)$ is nonzero. The transient absorption studies showed that NAGA does not affect the intersystem crossing rate, whereas Gd^{3+} enhances it. So taking k°_q as 0.0 for NAGA and 2.2×10^7 M^{-1} s^{-1} for Gd^{3+}, the plots of $\ln(1/\tau_q - 1/\tau_c - k^\circ_q [Q])$ *vs* $1/T$ shown in Figure 3b are linear. The frequency factors and activation energies derived from the slopes and intercepts are 4.3×10^9 M^{-1} s^{-1} and 2.7 kcal/mol for NAGA and 3.6×10^{12} M^{-1} s^{-1} and 6.0 kcal/mol for Gd^{3+}.

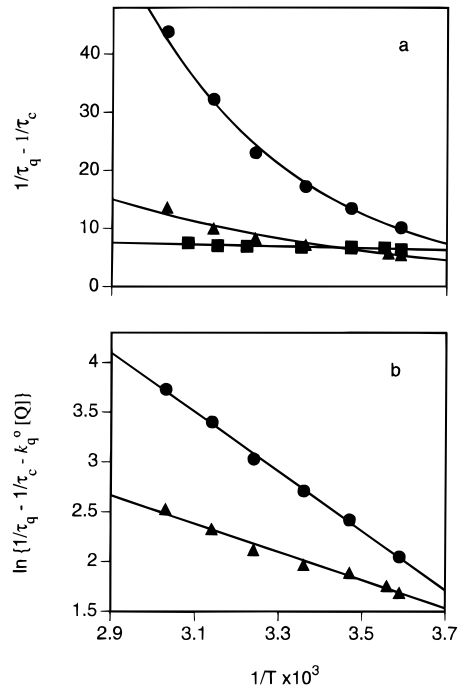

Figure 3. Temperature dependence of fluorescence lifetimes of 3-methylindole in the presence of (▲) NAGA, (■) ethyl acetate, and (●) Gd^{3+} analyzed using procedure III. (a) Line drawn to guide the eye. (b) Arrhenius plot of eq 11 with $k^\circ_q = 0.0$ for NAGA and 2.2×10^7 M^{-1} s^{-1} for Gd^{3+}.

Procedures II and III give very similar results for the temperature dependence of the nonradiative process due to these solute quenchers. The quenching by ethyl acetate has no detectable temperature dependence. The activation energies for NAGA and Gd^{3+} quenching are 2.5 ± 0.3 and 6.0 ± 0.5 kcal/mol in H_2O, respectively. Despite uncertainties in the procedures for determining the Arrhenius parameters, it is clear that the three types of quenchers have different temperature dependence. Frequency factors and activation energies of diffusion-controlled reactions in aqueous solution are about 10^{11} s^{-1} and 4 kcal/mol, in the range of values obtained here. However, the bimolecular quenching rate constants for NAGA, ethyl acetate, and Gd^{3+} are almost two orders of magnitude below the rate constant of a diffusion-controlled process. This allows us to associate the second temperature-dependent term in eq 7 directly with the solute-quenching process.

For comparison with the results from the analysis of the temperature dependence of the fluorescence lifetime with two Arrhenius terms (eq 9), the temperature dependence of Gd^{3+} quenching in H_2O was determined directly by measuring the bimolecular quenching rate constant k_q as a function of temperature between 5 and 50 °C. Stern−Volmer constants were obtained from relative fluorescence quantum yields using $GdCl_3$ concentrations from 0 to 0.3 M. The water quenching rate was held constant by adjusting the total ion concentration to 0.6 M using KCl. The lifetime in the absence of $GdCl_3$ was measured in 0.6 M KCl. K_{sv} ranged from 0.8 to 1.2 M^{-1} with a maximum around 25 °C. Figure 4a is the plot of k_q *vs* $1/T$. Figure 4b is the Arrhenius plot of $\ln(k_q - k^\circ_q)$ *vs* $1/T$, where k°_q is the temperature-independent bimolecular quenching rate due to intersystem crossing obtained from transient absorption experiments. The frequency factor and activation energy calculated from the intercept and slope are 5.8×10^{12} M^{-1} s^{-1}

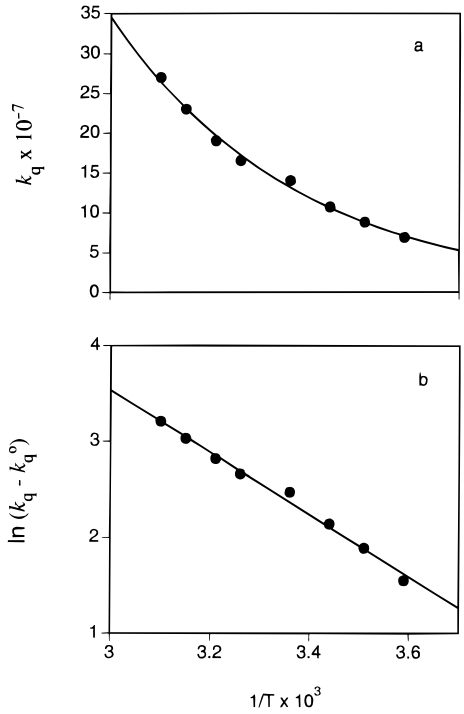

Figure 4. Temperature dependence of the Stern−Volmer rate constant for 3-methylindole fluorescence quenched by Gd^{3+}. (a) Line drawn to guide the eye. (b) Arrhenius plot with $k^\circ_q = 2.2 \times 10^7$ M^{-1} s^{-1}.

and 6.5 kcal/mol. These results agree well with the values of A_2 and E^*_2 in Table 3 from procedure II.

Finally, we measured the fluorescence lifetime of NATA in H_2O and D_2O as a function of temperature from 2 to 68 °C. The lifetime of NATA in H_2O at 25 °C is 3 ns, compared to 8.2 ns for 3-methylindole. The shorter lifetime for NATA is due mostly to intramolecular quenching by amides. The temperature data set was fit by global analysis to eqs 8 and 9 assuming one and two temperature-dependent terms (Table 3). The analysis for one temperature-dependent term gave $k_o = 17 \times 10^7$ s^{-1} and $E^*_1 = 6.9$ kcal/mol in H_2O with $\chi_r^2 = 2.4$. Kirby and Steiner[33] obtained $k_o = 15 \times 10^7$ s^{-1} and $E^*_1 = 6.6$ kcal/mol from the temperature dependence of the fluorescence quantum yield. The analysis for two temperature-dependent terms gave a better fit with $\chi_r^2 = 1.9$. The first temperature-dependent term has an activation energy $E^*_1 = 12.6$ kcal/mol and a 2.8-fold deuterium isotope effect, which is characteristic of water quenching in indole derivatives. Water quenching in NATA is masked when temperature-dependent data are fit to a single Arrhenius term, but clearly resolved when two Arrhenius terms are used. The activation energy $E^*_2 = 3.2$ kcal/mol of the second temperature-dependent term is very similar to the value for intermolecular quenching of 3-methylindole by NAGA. Petrich et al.[16] calculated the activation energy for intramolecular quenching in NATA using a two-step method similar to procedure III. These authors constructed an Arrhenius plot by subtracting the total nonradiative rate of 3-methylindole from that of NATA and obtained a value of 5.6 kcal/mol. Their method assumes that the intersystem crossing and water quenching rates are the same for 3-methylindole and NATA. Our triplet yield measurements show that the intersystem crossing rate of NATA is 2.4 times higher than that of 3-methylindole. The water quenching rate k_{si} calculated for NATA from A_1 and E^*_1 is about half the value of k_{si} in 3-methylindole.

(33) Kirby, E. P.; Steiner, R. F. *J. Phys. Chem.* **1970**, *74*, 4480−4490.

Conclusion

In this paper, we have shown that the peptide bond quenches indole fluorescence. Transient absorption experiments indicate that the peptide group does not affect the intersystem crossing rate. Peptide quenching is weakly temperature dependent. This argues against enhancement of internal conversion as the quenching mechanism, because internal conversion is usually independent of temperature.[32] Two other types of quenchers, ethyl acetate and Gd^{3+}, have distinctly different activation energies. All three quenchers are thought to quench indole fluorescence primarily by electron transfer. For an electron-transfer quenching process, the quenching rate and activation energy are related to the reduction potential of the electron acceptor and the reorganization energy,[34−36] which are expected to depend on the compound and solvent.

An electron transfer quenching mechanism for the peptide bond is also supported by the relative quenching rates of the class three compounds. The amide group is electron withdrawing. The presence of a second amide will enhance the electrophilicity of the first amide through the inductive effect, thereby increasing the quenching rate. The inductive effect will be larger and the quenching rate higher when the two amides are closer together. Carboxylate is not an electron withdrawing group and will not have an inductive effect on amide. The three classes of compounds show the expected trends. First, two amides are required for detectable quenching. Second, the quenching rate constants of *N*-acetylglutamine, *N*-acetylasparagine, and malonamide are in the expected order: $2.2 \times 10^7 < 8.8 \times 10^7 < 33 \times 10^7$ M^{-1} s^{-1}. The major structural difference among these compounds is the distance between the two amides: three methylene groups for *N*-acetylglutamine, two for *N*-acetylasparagine, and only one for malonamide. For amide compounds containing electron-withdrawing substituents such as the chloro group, the quenching may occur via a different pathway and yet still involve electron transfer. For example, chloroform is a good quencher itself. The quenching mechanism may be

$$RCl + e^- \rightarrow R^\bullet + Cl^-$$

and quenching may be very efficient. Eberson[37] has done an extensive study of this type of reaction.

In favorable cases, the temperature dependence of the fluorescence lifetime can be used to calculate the rates of individual nonradiative processes. A global analysis program that fits the entire data set directly to a temperature-dependent physical model makes it possible to distinguish two temperature-dependent processes with distinct activation energies. A second temperature-dependent term in addition to water quenching is clearly resolved for both inter- and intramolecular quenching of indoles. Therefore, the rate constants of these two quenching processes can be determined from the Arrhenius parameters. Possible temperature-independent processes include fluorescence emission, intersystem crossing, and internal conversion. The radiative rate k_r and intersystem crossing rate k_{isc} can be determined independently from fluorescence quantum yield and triplet quantum yield measurements. So far there is no experimental evidence for internal conversion in indoles in aqueous solution. Values of $k_r + k_{isc}$ are compared with k_o calculated from the temperature dependence of the fluorescence lifetime in Table 2. Using $k_o = 9.8$

(34) Marcus, R. A. *Annu. Rev. Phys. Chem.* **1964**, 155−196.
(35) Rehm, D.; Weller, A. *Isr. J. Chem.* **1970**, *8*, 259−271.
(36) Marcus, R. A.; Sutin, N. *Biochim. Biophys. Acta* **1985**, *811*, 265−322.
(37) Eberson, L. *Acta. Chem. Scand. B* **1982**, *36*, 533−543.

$\times 10^7$ s^{-1} from procedure II for NATA (Table 3), the values of $k_r + k_{isc}$ and k_o are virtually identical for 3-methylindole, indole, *N*-methylindole, and NATA. Two conclusions can be drawn: (1) k_{isc} is independent of temperature. (2) The temperature-independent processes in aqueous solution are radiation and intersystem crossing. Therefore, if the k_o value obtained from the temperature dependence of the fluorescence lifetime is much larger than $k_r + k_{isc}$ determined separately from quantum yield measurements, then there must be another temperature-independent process.

The fluorescence decay of tryptophan in proteins is usually multiexponential with lifetimes ranging from several hundred picoseconds to 10 ns.[38] The lifetime heterogeneity is due to ground-state heterogeneity comprising multiple microconformational states with different proximity and orientation of the indole chromophore to protein functional groups. Peptide bonds plus water molecules are the two most likely quenchers of indole fluorescence in proteins. The intramolecular peptide quenching rate in NATA at 25 °C calculated from $k_q = A_2 \exp(-E^*_2/RT)$ using the Arrhenius parameters in Table 3 is 2.0×10^8 s^{-1}. The peptide quenching rate may vary considerably due to neighboring amide and peptide groups. In contrast, the water quenching rate k_{si} in NATA is only 3.4×10^7 $s^{-1.}$ Thus, we expect that peptide quenching has a major influence on the fluorescence lifetime in proteins. The intramolecular peptide quenching rate may be extracted from the temperature dependence of the fluorescence lifetime as long as the conformation of the protein does not change appreciably in the temperature range examined. Proton transfer may also play a role in protein fluorescence if the indole chromophore can access a good proton donor. Intersystem crossing appears to be insensitive to protein functional groups and may not vary with environment in the absence of a heavy atom. The intersystem crossing rate of NATA and tryptophan is 5×10^7 s^{-1}. In the five indole derivatives studied, k_{isc} ranges from 2.1×10^7 to 7.6×10^7 s^{-1}, presumably reflecting substituent effects.

Strictly speaking, the results in this paper are applicable to surface tryptophans exposed to aqueous solvent. Nevertheless, it is tempting to speculate about the implications for buried tryptophans. Water quenching no longer occurs in the protein interior. The fluoresence of buried tryptophans is weakly temperature dependent,[39,40] consistent with peptide quenching. The multiple lifetimes of a buried tryptophan could be explained by different microconformational states of the indole ring with respect to nearby peptide and amide groups. The intersystem crossing rate of tryptophan in the protein interior should be similar to the value in water. The intersystem crossing rate of indole in cylcohexane calculated from triplet yield[28] and lifetime[33] data is 8.2×10^7 s^{-1}, which is close to k_{isc} in water.

Acknowledgment. This work was supported by NIH grant GM42101. We thank Dr. J. M. Beechem for providing the global deconvolution program for analyzing the lifetime data according to eq 9.

JA961307U

(38) Beechem, J. M.; Brand, L. *Annu. Rev. Biochem.* **1985**, *54*, 43−71.
(39) Kim, S.-J.; Chowdhury, F. N.; Stryjewski, W.; Younathan, E. S.; Russo, P. S.; Barkley, M. D. *Biophys. J.* **1993**, *65*, 215−226.
(40) Pepmiller, C.; Bedwell, E.; Kuntz, R. R.; Ghiron, C. A. *Photochem. Photobiol.* **1983**, *38*, 273−280.